Proposed Triaxial Atomic Force Microscope Contact Free Tweezers for Nanoassembly

Triaxial Atomic Force Microscope Contact-Free Tweezers for Nanoassembly

Keith A Brown[1] **and Robert M Westervelt**[1,2]

[1]School of Engineering and Applied Science, Harvard University, Cambridge, MA 02138, USA

[2]Department of Physics, Harvard University, Cambridge, MA 02138, USA

E-mail: `westervelt@seas.harvard.edu`

Abstract. We propose a Traixial Atomic Force Microscope (AFM) Contact-free Tweezer (TACT) for the controlled assembly of nanoparticles suspended in a liquid. The TACT overcomes four major challenges faced in nanoassembly: (1) The TACT can hold and position a single nanoparticle with spatial accuracy smaller than the nanoparticle size ($\sim$ 5 nm). (2) The nanoparticle is held away from the surface of the TACT by negative dielectrophoresis (nDEP) to prevent van der Waals forces from sticking it to the TACT. (3) The TACT holds nanoparticles in a trap that is size-matched to the particle and surrounded by a repulsive region so that it will only trap a single particle at a time. (4) The trap can hold a semiconductor nanoparticle in water with a trapping energy greater than thermal energy. For example, a 5 nm radius silicon nanoparticle is held with 10 k_BT at room temperature. We propose methods for using the TACT as a nanoscale pick-and-place tool to assemble semiconductor quantum dots, biological molecules, semiconductor nanowires, and carbon nanotubes.

PACS numbers: 81.16.-c and 68.37.Ps

1. Introduction

The controlled assembly of nanoscale components is a grand challenge in nanotechnology. Advances in growth and synthesis have enabled the reliable fabrication of homogenous nanoparticles with diverse properties[1, 2]. However, these particles are typically suspended in a liquid and are difficult to assemble into devices or circuits. To realize the potential for new classes of nanoelectronic and photonic systems, methods to controllably assemble nanoparticles need to be developed. Self-assembly techniques have proved to be useful in creating complex regular structures[3, 4], but to progress to irregular electronic or photonic structures, controlled assembly is needed.

1.1. Semiconductor Quantum Dots

Colloidal semiconductor quantum dots provide a rich quantum system that can be controllably synthesized to have specified physical properties. Quantum dots have been created from II-VI Semiconductors such as CdSe[5], III-V semiconductors such as InAs[6], group IV semiconductors such as Si[7], and IV-VI semiconductors such as PbSe[8]. Nanoparticles with diameters ranging from 1 to 10 nm have been grown with monodispersity in diameter of 5 to 10%. A second semiconductor layer can be epitaxially grown around a quantum dot to greatly improve its photoluminesce properties[9, 10]. Branched heterostructures of specified geometries may be grown by controlling the growth precursors[11].

Controlled assembly of quantum dots could lead to the realization of novel electronic and photonic devices. Multiple quantum dots have been incorporated into electronic systems to create field effect transistors and dynamic memory[12]. Single quantum dots have been electrically contacted to create single electron transistors[13]. Such systems can be coupled with an external magnetic field to create transistors which do operations on single electrons based on their spin. Such devices could be coupled together for spintronics systems[14]. Multiple quantum dots and dot arrays have been incorporated into photonic systems to create light emitting diodes[15] and lasers[16]. Single quantum dots can be used to create systems in which a single exciton is strongly coupled to a photon in a demonstration of cavity quantum electrodynamics (CQED). This has been demonstrated in epitaxially grown quantum dots[17, 18, 19]. The controlled assembly of single quantum dots can enable multiple interacting CQED structures.

1.2. Controlled Assembly

Controlled assembly is the deliberate placement of specific objects in a desired location and it is necessary for constructing non-regular structures. Extending controlled assembly to nanoscale biological, electrical, and optical structures has been the focus of much recent work using a variety of approaches[20, 21]. Micro-mechanical grippers have been constructed as pick-and-place tools by operating in a scanning electron microscope[22]. Microgrippers rely on physical contact so van der Waals (vdW) forces

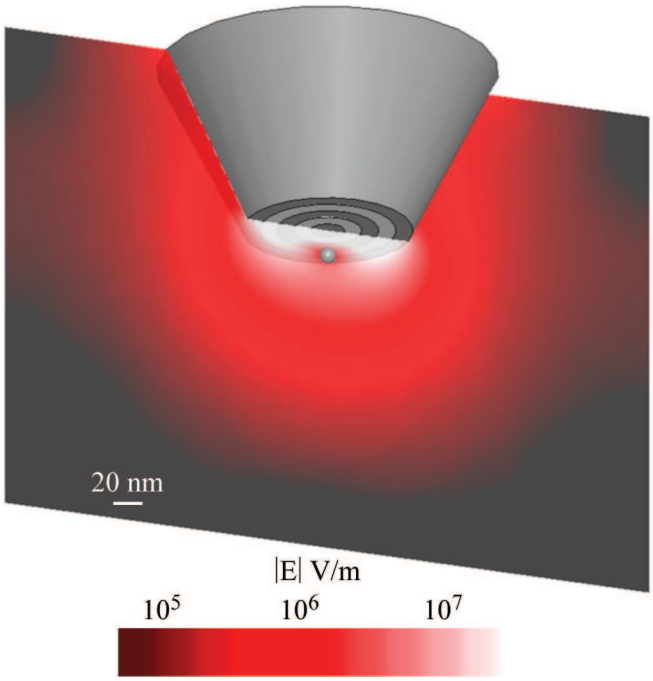

Figure 1. Illustration of a Triaxial AFM Contact-free Tweezer (TACT) trapping a 5 nm radius silicon sphere suspended in water using negative dielectrophoresis (nDEP). The center electrode is a conducting AFM probe that has been coated with alternating insulating and conducting layers. Radio frequency voltages are applied to the inner two electrodes which generate an electric field whose magnitude is denoted by the color scale. The silicon nanoparticle is trapped in the zero of the field created displaced from the tip.

limit their ability to manipulate objects smaller than 10 μm[23]. Optical tweezers can trap 10 nm to 10 μm objects suspended in a liquid without contact and are extensively used for micro- and nanoassembly[24, 25]. Atomic Force Microscopes (AFMs) are well suited to probe the nanoscale because of their inherent nanometer precision and force-sensing capability. For these reasons, AFMs have been used to mechanically position nanoparticles on surfaces[20] and pattern molecules on surfaces with dip-pen nanolightgraphy[26]. Dielectrophoresis (DEP) using micro- or nano-fabricated stationary electrodes is also a very useful tool for micro-[27] and nano-manipulation[32].

To controllably assemble nanoscale components, four challenges must be overcome: (1) The object must be trapped and placed with spatial accuracy comparable to its size. This means that the trap must be size-matched to the object and positioned with nanometer precision. (2) Van der Waals forces will adhere nanoparticles to any surface. Nanoparticles must therefore be picked up and held without physical contact. (3) One nanoparticle should be held at a time, which limits the utility of entirely attractive methods like positive dielectrophoresis (pDEP) that cause clustering of many nanoparticles. (4) The energy barrier the particle must overcome to escape the trap must be greater than k_BT to hold the particle against Brownian motion.

In this work, we present a Triaxial AFM Contact-free Tweezer (TACT) that is capable of the nanoassembly of single nanoparticles suspended in a fluid, as shown schematically in figure 1. The TACT is formed by three coaxial electrodes at the tip of an AFM probe that can trap particles without contact using negative dielectrophoresis (nDEP). The TACT overcomes each of the previously presented challenges facing nanoscale controlled assembly: (1) The size of the trap is dictated by device fabrication and can be size-matched to the desired nanoparticle. Nanometer resolution positioning of the trap is afforded by the AFM. (2) The nanoparticle is picked out of a liquid suspension and held away from the tip with nDEP so it does not touch any surfaces until it reaches its destination. (3) The nanoparticle-sized potential well created by the TACT is surrounded by a repulsive region which ensures that only one particle will be trapped at a time. (4) The trap created by the TACT is strong enough to hold a 5 nm radius silicon sphere in water with greater than 10 k_BT at room temperature.

2. Dielectrophoresis of Semiconductor Nanoparticles

Dielectrophoresis (DEP) is a very useful tool for micro-[27] and nano-manipulation[32]. Dielectrophoresis is the interaction of a dielectric object with a non-uniform electric field. The field induces an electric dipole moment $\vec{p}$ which gains energy from the electric field $U_{DEP} = -\vec{E} \cdot \vec{p}$. The energy gained by a spherical dielectric particle of radius r and dielectric constant ϵ_P in an electric field $\vec{E}$ at frequency ω is given by[33],

$$U_{DEP} = -2\pi r^3 K(\omega) \epsilon_M |\vec{E}|^2, \tag{1}$$

where ϵ_M is the permittivity of the medium and $K(\omega)$ is the Clausius-Mossotti factor,

$$K(\omega) = Re\left[\frac{\tilde{\epsilon}_P - \tilde{\epsilon}_M}{\tilde{\epsilon}_P + 2\tilde{\epsilon}_M}\right]; \tag{2}$$

$\tilde{\epsilon_P}$ and $\tilde{\epsilon_M}$ are the complex dielectric constants of the particle and medium. The Clausius-Mossotti factor ranges from 1 to -0.5 and specifies the character of the DEP force. If $\tilde{\epsilon}_P > \tilde{\epsilon}_M$, the particle will be attracted to the local field maximum with positive dielectrophoresis (pDEP). If $\tilde{\epsilon}_P < \tilde{\epsilon}_M$, the particle will be pushed towards the local field minimum with negative dielectrophoresis (nDEP). Radio frequency (RF) voltages at frequencies between 10 kHz and 100 MHz are preferable for DEP because they avoid electrophoresis, electroosmotic flow, electrochemistry, dielectric heating, and the effects of ionic screening[27]. The strength of DEP depends on the magnitude of the applied electric field. The maximum electric field possible in a suspension is given by the dielectric breakdown of the liquid. The breakdown field of water depends on electrode geometry and the duration of the field; typically the breakdown field exceeds 1 MV/cm[28].

Van der Waals (vdW) forces adhere nanoparticles strongly to surfaces, so unwanted contact must be avoided for successful nanoassembly. The magnitude of the vdW force acting on a sphere near a plane is proportional to the radius of the sphere[29] while the DEP force is proportional to the volume of the sphere. As the radius of the particle

is decreased, the vdW force will become more important relative to DEP. For a 5 nm radius semiconductor nanoparticle†, both the maximum DEP force and typical vdW force are ~ 20 pN.

Negative dielectrophoresis is well suited for the assembly of nanoparticles because it can prevent them from contacting any surfaces. A consequence of Maxwell's equations is that without a time varying magnetic field, the electric field can only have maxima where there is net charge. This restriction means that electric field maxima cannot be displaced from electrodes. Since pDEP attracts particles to electric field maxima, pDEP cannot be used for non-contact trapping without additional forces[34]. It is, however, possible to create a small isolated zero in the electric field. Negative dielectrophoresis pushes particles into local electric field minima and therefore can be used to trap particles without bring them into contact with surfaces.

Semiconductor nanoparticles in water are ideal candidates for manipulation with nDEP. The typical static dielectric constant of semiconductors varies between $8\epsilon_0$ and $14\epsilon_0$[30]. Water has a static dielectric constant of $78.4\epsilon_0$, constant within 1% between DC and 300 MHz[35]. We use silicon as a typical semiconductor; its dielectric constant is $\epsilon_P = 12\epsilon_0$ and Clausius-Mossotti factor in water is $K = -0.4$ between $0.1 - 100$ MHz. A K of nearly the minimum possible $K = -0.5$ indicates that nDEP will act strongly on semiconductors in water.

3. Nanoassembly with Triaxial AFM Contact-free Tweezers

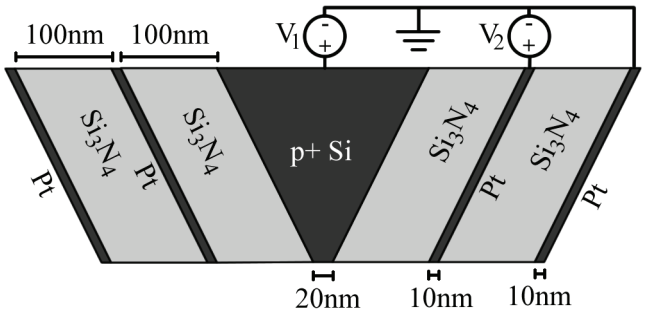

Figure 2. The Triaxial AFM Contact-free Tweezer (TACT) geometry used in the electric field simulations. The center p+ Si electrode is held at V_1, the middle Pt electrode is held at V_2, and the outer Pt electrode is grounded. The electrodes are separated by 100 nm layers of silicon nitride.

We propose a Triaxial AFM Contact-free Tweezer (TACT) that can trap a single semiconductor nanoparticle suspended in water. The TACT is comprised of three independently contacted coaxial electrodes constructed on an AFM probe as shown

† The nanoparticle is taken to have $\epsilon_P = 10\epsilon_0$[30], a Hamaker constant of 5×10^{-20} J in water[31], subject to a field that varies between 0 to 1 MV/cm in one particle diameter, and be located 0.5 nm from a substrate of the same material.

in figure 2. The TACT can be fabricated by depositing an insulator on a conducting AFM probe followed by a conducting layer and another pair of insulating and conducting layers. The tip is etched to expose the triaxial electrodes. The inner electrode is held at voltage V_1, the middle electrode is held at V_2 and the outer electrode is grounded. The electric field generated by the TACT is calculated by 2D (Maxwell SV - Ansoft Corp.) and 3D (Maxwell 11 - Ansoft Corp.) finite element electrostatic simulations. This system may be treated using a quasistatic approximation because all length scales are much shorter than the wavelength of the applied electromagnetic field[36]. Data analysis was performed in MATLAB (The MathWorks, Inc.).

The TACT can use nDEP to trap nanoparticles much smaller than the tip radius without bringing them into contact with the surface of the tip. Figure 3(a) shows the magnitude of the electric field calculated near the apex of the TACT. There is a zero in the electric field displaced from the tip by $z_0 = 44$ nm. The right and bottom insets show the trapping energy calculated using equation (1) for a 5 nm radius silicon sphere along the z-axis at $r = 0$ and along the r-axis at $z = z_0$. The energy minima forms a trap that can hold a single nanoparticle. The trap is weakest along the z-axis making it where a particle is most likely to escape. The maximum energy on this axis defines the trapping energy U_{trap} located at z_{trap}. The trapping energy U_{trap} for a 5 nm radius silicon sphere is greater than 10 k_BT at room temperature, meaning that it will be held against Brownian motion.

Nanoparticles outside the trapping region are pushed away by a repulsive force. The force $\vec{F}$ experienced by a 5 nm radius silicon sphere is plotted as a vector field superimposed on the magnitude of the electric field in figure 3(b). The dashed line indicates a region inside which $\vec{F}$ pushes toward the trap. Outside this region, $\vec{F}$ points away from the trap. The dashed line follows a ridge in the potential landscape with a saddle point located on the z-axis at z_{trap}. At small length scales, fluid flows are laminar so $\vec{F}$ can be converted to the nanoparticle velocity $\vec{v}$ by Stokes' law, $\vec{F} = 6\pi\mu r\vec{v}$ where μ is the fluid viscosity[37]. Stokes' law implies that the vector field in figure 3(b) also represents $\vec{v}$ so particles inside the trapping region will be pushed along streamlines to the minimum while particles outside the trapping region will be pushed away from the TACT.

The TACT acts as a movable hand that can grasp a single suspended particle and release it at a desired location. The repulsive region around the trap combined with the ability to tune the size of the trap makes TACT assembly analogous to a person grabbing a baseball out of a bag full of baseballs. The character of the trap is varied from attractive to repulsive by sweeping the ratio of applied voltages V_1/V_2.

An example of the assembly procedure is as follows:

I. A topographic scan is taken with the AFM to locate the destination of the nanoparticle.

II. The TACT is made repulsive repulsive by setting $V_2 = 0$ V, as shown in figure 4(g). The inner voltage V_1 is held at $V_1 = V_2 - 10$ V throughout the assembly procedure.

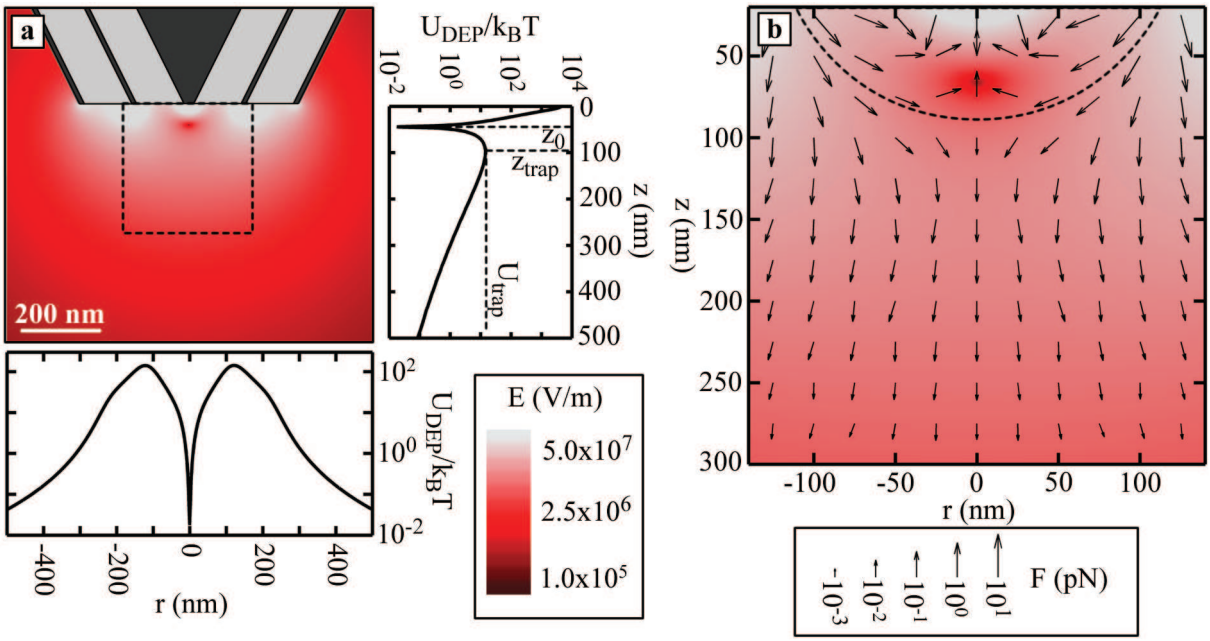

Figure 3. (a) The electric field calculated by a 2D simulation with $V_1 = 0$ and $V_2 = -10$ V. (right) The dielectrophoretic energy U_{DEP} of a 5 nm radius silicon sphere in water is calculated in units of thermal energy at room temperature from equation (1) along z with $x = 0$. The minima of U_{DEP} at $z > 0$ is the location of the trap z_0. The maximum energy U_{trap} beyond the trap, $z_{trap} > z_0$, determines the strength of the trap. For a 5 nm radius silicon sphere U_{trap} is greater than 10 k_BT. (bottom) Trapping energy U_{DEP} is calculated in units of thermal energy at room temperature as a function of x at $z = z_0$. (b) The force $\vec{F}$ experienced by a 5 nm radius silicon sphere calculated from a 3D simulation is vector plotted with the electric field magnitude denoted by the color scale. The location of this plot corresponds to the dashed box in (a). The region separated by the curved dashed line represents the attractive region of the trap while the rest is repulsive.

III. The tip is moved into a liquid suspension of the desired nanoparticles.

IV. A trap is formed by increasing V_2 which draws an electric field zero towards the TACT, as shown in figure 4 (g)→(a). The repulsive region folds around the trap like a hand grabbing a baseball. Matching the size of the TACT to the size of the nanoparticle ensures that only one nanoparticle can be trapped at a time. In the case of fluorescent particles such semiconductor quantum dots, fluorescence microscopy can be used to determine if a particle is present.

V. The TACT is moved to the desired location and V_2 is returned to 0 V. The spatial profile of the field progresses from figure 4 (a)→(g) pushing the particle onto the surface where it is held with vdW forces.

Using this procedure, the particle can be deposited on a substrate while never touching the TACT and risking being stuck to it by vdW forces.

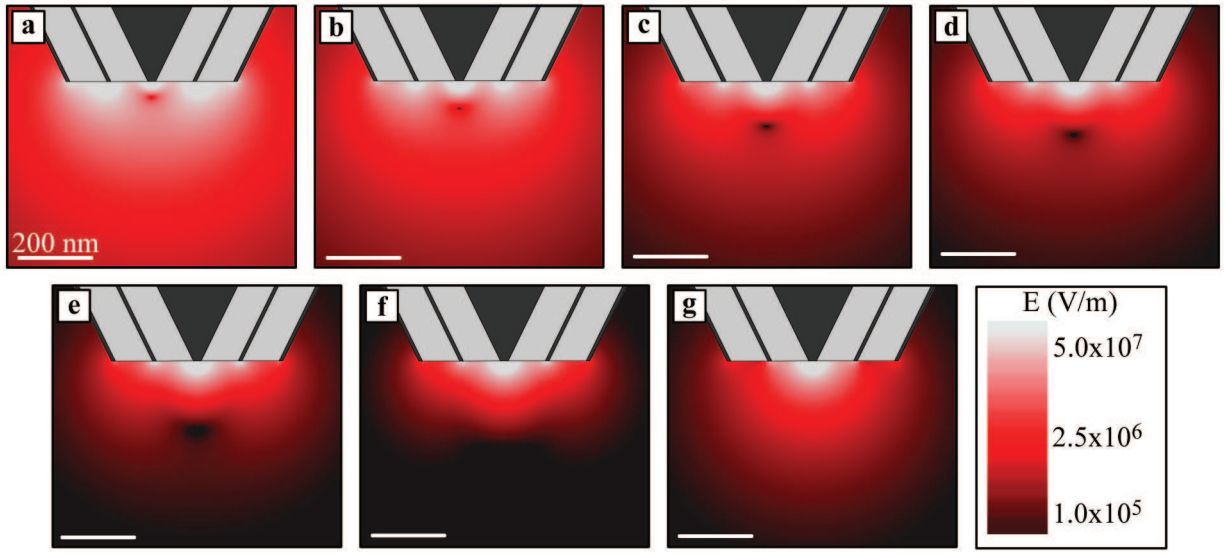

Figure 4. Electric field calculated by 2D simulation near the tip of the TACT while varying V_2 and holding $V_1 = V_2 - 10$ V. (a) $V_2 = 10$ V, (b) $V_2 = 5$ V, (c) $V_2 = 2.9$ V, (d) $V_2 = 2$ V, (e) $V_2 = 1.5$ V, (f) $V_2 = 1.2$ V, and (g) $V_2 = 0$ V.

4. Analytic Model of the TACT

We have developed a model to analyze the spatial profile of the electric field generated by the TACT to illuminate its potential for trapping nanoparticles. The geometry of the TACT can be approximated by three simple electrodes: two concentric rings in the x-y plane centered around a disc at the origin, as shown in figure 5(a). This approximation is most valid in the region close to the end of the tip where the the conical probe has little effect. The radius of the inner ring is R and the radius of the outer ring is $2R$. We give the rings and disc a thickness δ for the purpose of assigning them capacitances, but we take $\delta \ll R$ so the fields generated by the electrodes are well approximated by those of a point charge at the origin and rings of infinitesimal thickness. The charge on a given electrode can be given in terms of the voltages V_i and capacitance matrix C_{ij} where $i = 1$ or $j = 1$ corresponds to the center disc, 2 represents the middle ring, and 3 represents the outer ring. The charge on a given electrode q_i is given by,

$$q_1 = C_{12}\,(V_1 - V_2) + C_{13}V_1, \tag{3}$$

$$q_2 = -\,C_{12}\,(V_1 - V_2) + C_{23}V_2, \tag{4}$$

$$q_3 = -\,C_{13}V_1 - C_{23}V_2. \tag{5}$$

The model is simplified by defining four dimensionless parameters, $\kappa_1 = C_{12}/C_{23}$, $\kappa_2 = C_{13}/C_{23}$, $\xi = z/R$, and $\eta = V_1/V_2$. The z-component of the electric field on the z-axis generated by these electrodes is,

$$E_z = \frac{C_{23}\Delta V}{4\pi\epsilon_0 R^2}\frac{1}{(1-\eta)} \times$$

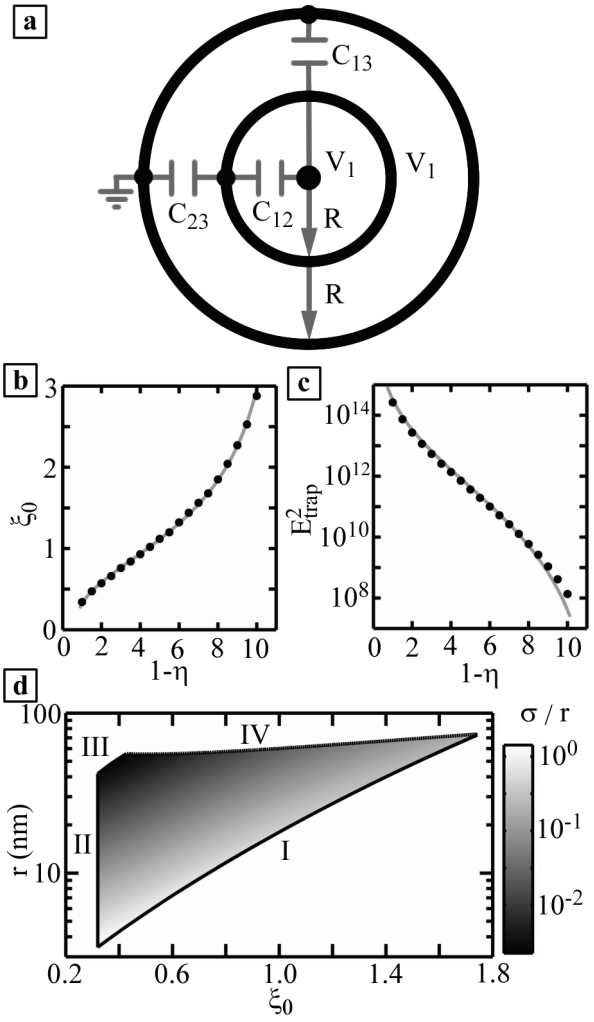

Figure 5. (a) Schematic of the ring electrode model of the TACT. The electrodes lie in the x-y plane with the center electrode at the origin. (b) normalized location $\xi_0 = z_0/R$ of the electric field zero versus voltage ratio $1-\eta = (V_2-V_1)/V_2$. The points correspond to results from finite element simulation while the line is the prediction of the ring model, fit to the points. (c) The square of the maximum value of the electric field E_{trap} at z_{trap} versus $1-\eta$. The points are from the finite element simulation and the line is the prediction from the ring model, fit to the points. (d) Representation of the region in which the TACT can trap a silicon nanoparticle with radius r held at ξ_0. The smallest Si particle that can be held against thermal energy k_BT with the TACT is $r = 2$ nm. The shading corresponds to the root mean square displacement σ/r of the particle along the z-axis in the trap normalized by its radius which is calculated by linearizing E_z about z_0.

$$\left[\frac{\kappa_1(\eta-1)+\kappa_2\eta}{\xi^2}+\frac{(1-\kappa_1(\eta-1))\,\xi}{(\xi^2+1)^{3/2}}-\frac{(1+\kappa_2\eta)\,\xi}{(\xi^2+4)^{3/2}}\right], \tag{6}$$

where $\Delta V = V_2 - V_1$. The maximum ΔV possible without dielectric breakdown of water is $\Delta V = 10$ V for the case of insulators that are 100 nm thick.

The normalized location $\xi_0 = z_0/R$ of the electric field zero is determined by the

voltage ratio $\eta = V_1/V_2$, as shown in figure 5(b). The voltage ratio η necessary to produce a given ξ_0 is found by setting equation (6) equal to zero. To obtain the ring radius R and relative values of the capacitance matrix C_{ij}, we fit the solutions of equation (6) to values of z_0 and $1-\eta$ obtained from finite element simulations of the electric field. Figure 5(b) shows excellent agreement in the fit between the analytic solution (curve) and the finite element simulation (points). The fit yields $\kappa_1 = 0.025 \pm 0.001$, $\kappa_2 = 0.063 \pm 0.001$ and $R = 130 \pm 2$ nm for the tip geometry shown in figure 2(b).

The magnitude of the trapping electric field E_{trap} that determines the energy barrier U_{trap} of the trap is specified by the voltage ratio $\eta = V_1/V_2$ as shown in figure 5(c). The location $\xi_{trap} = z_{trap}/R$ of the smallest magnitude electric field E_{trap} on the barrier surrounding the zero can be obtained by numerically solving $dE_z/dz = 0$. To obtain the absolute values of the capacitance matrix C_{ij}, we fit E_{trap} from equation (6) to values of E_{trap} and $1 - \eta$ obtained from finite element simulations of the electric field. Figure 5(b) shows good agreement in the fit between the analytic solution (curve) and the finite element simulation (points). The fit yields $C_{23} = 12.0 \pm 0.5$ aF and deviates at large values of $1 - \eta$, because it is not possible to neglect the influence of the conical probe far away from the tip. The value of E^2_{trap} can be used together with equation (1) to calculate the trapping energy U_{trap} of a given particle.

The TACT provides a powerful way to trap and assemble particles of a range of sizes. The region in which the TACT can trap a silicon nanoparticle as a function of trap location ξ_0 and nanoparticle radius r is given by boundaries I, II, III, and IV shown in figure 5(d).

I. This boundary is determined by the condition that the trapping energy U_{trap} be greater than thermal energy k_BT.

II. The minimum trap location ξ_0 is given by the breakdown voltage between the middle and outer electrodes.

III. The radius of the trapped particle r cannot be larger than z_0 without the particle coming into contact with the tip.

IV. The particle cannot be larger than the trap size. This is estimated by limiting the particle radius $r < z_{trap} - z_0$.

This analysis predicts that silicon particles with radius as small as 2 nm can be trapped with the TACT. This model is most valid when r is small compared to the physical size of the trap.

It is possible to trap particles with the TACT so that their random fluctuations due to Brownian motion are smaller than their radius. We estimate how tightly particles are held by linearizing E_z about z_0 which gives U_{DEP} parabolic in z. This approximation defines a spring constant $k \propto (dE_z/dz)^2$ which can be used with the equipartition theorem to approximate the root mean displacement σ in z as,

$$\sigma = \left(\langle (z - z_0)^2 \rangle\right)^{1/2} = \left(\frac{-k_BT}{4\pi r^3 \epsilon_M K \left(dE_z/dz\right)^2}\right)^{1/2}. \tag{7}$$

This number will be real because K is a negative number for nDEP. The root mean square displacement σ normalized by the particle radius is shown as a gray scale versus r and ξ_0 in figure 5(d). All but the smallest particle radius have $\sigma < r$. We only consider fluctuations on the z-axis because that is the most likely direction of escape.

Physically smaller TACTs can trap objects more tightly. Electric field simulations were performed with TACT geometries scaled by a factor β. Comparison of the analytic model to these simulations reveals that $C_{ij} \propto \beta$ and $R \propto \beta$. The maximum voltage difference $\Delta V \propto \beta$ because it is picked to limit the electric field between the electrodes to less than the field necessary to cause dielectric breakdown of the water. The trap location ξ_0 does not depend on β because the relative capacitances κ_1 and κ_2 do not change with β. The curves in figures 5 (b) and (c) and boundaries I and II in figure 5(d) are therefore independent of β and universal to the TACT. Consequentially, reducing the physical size of the TACT does not enable trapping smaller objects. Increasing the physical size of the TACT does enable trapping larger particles because the locations in r of boundaries III and IV scale with β. Smaller TACTs will trap objects with smaller thermal fluctuations because the scaling of σ in equation (7) reveals that $\sigma \propto \beta$.

5. Possible Applications

The TACT enables nanoassembly of single semiconductor quantum dots onto substrates. Semiconductor quantum dots such are ideal candidates for manipulation with the TACT because their diameter is typically 1 to 10 nm and their dielectric constant $\epsilon_P \sim 10\epsilon_0$ is much less than that of water $\epsilon_M \sim 78\epsilon_0$. The quantum dots may be selected based on characteristics such as photoluminescence spectrum, then positioned on pre-fabricated nanostructures to create complex interacting electronic and photonic systems. Nanoscale alignment with the substrate is afforded by the AFM and single-particle trapping and holding is granted by the TACT.

This technique is also well suited for manipulation of small biological molecules such as proteins. By selecting a frequency above the β relaxation of the protein, typically $1 - 10$ MHz, the protein is no longer able to rotate with the applied field and will have a dielectric constant smaller than that of water[38, 39, 40]. The ability to trap and hold single proteins could enable single molecule experiments and single molecule patterning.

The TACT geometry can be modified to manipulate semiconductor nanowires which are candidates for for nanoelectronics, photonics, spintronics, and quantum information[41, 42]. A chisel shaped AFM probe can be used to create an elongated trap which is well suited to hold nanowires or carbon nanotubes. The electrode spacing can be modified from what is presented here to obtain the optimum trap shape. Smaller radius tips would have better spatial resolution as an AFM while larger tips would allow for trapping of larger particles.

6. Conclusions

We have proposed triaxial AFM contract-free tweezers, a novel nanoassembly tool capable of positioning nanoscale components as small as 2 nm suspended in liquid. The TACT overcomes the challenges inherent to nanoassembly by: (1) Matching the size of the trap to that of the desired nanoparticle and using the AFM for nanometer precision in positioning. (2) Using nDEP to hold the particle without contact, avoiding vdW forces from sticking the particle to the tip. (3) Surrounding the trap with a repulsive region to prevent clustering of particles. (4) Holding particles with radius of 2 nm or greater with a trapping energy greater than k_BT at room temperature to control Brownian motion. The combination of these abilities enable a nanoscale pick-and-place tool. We have investigated the TACT with electrostatic simulations and analyzed the electric field it generates using a ring electrode model. The model provides analytical expressions for the trap location and reveals the particle sizes that can be held with the TACT. We also propose methodology for trapping semiconductor nanowires, carbon nanotubes, and biological molecules.

Acknowledgments

We acknowledge support by the Department of Defense through the National Defense Science & Engineering Graduate Fellowship (NDSEG) Program and the National Cancer Institute MIT-Harvard Center of Cancer Nanotechnology Excellence.

References

[1] Murray C B, Kagan C R and Bawendi M G 2000 *Annu. Rev. Mater. Sci.* **30** 545
[2] Huang Y, Duan X, Cui Y, Lauhon L J, Kim K-H and Lieber C M 2001 *Science* **294** 1313
[3] Shin S K, Yoon H-J, Jung Y J and Park J W 2006 *Curr. Opin. Chem. Biol.* **10** 423
[4] Medintz I L, Uyeda H T, Goldman E R and Mattoussi H 2005 *Nat. Mater.* **4** 435
[5] Murray C B, Norris D J and Bawendi M G 1993 *J. Am. Chem. Soc.* **115** 8706
[6] Guzelian A A, Banin U, Kadavanich A V, Peng X and Alivisatos A P 1996 *Appl. Phys. Lett.* **69** 1432
[7] Brus L E, Szajowski P F, Wilson W L, Harris T D, Schuppler S and Citrin P H 1995 *J. Am. Chem. Soc.* **1995** 2915
[8] Wehrenberg B L, Wang C and Guyot-Sionnest P 2002 *J. Phys. Chem. B* **106** 10634
[9] Peng X, Schlamp M C, Kadavanich A V and Alivisatos A P 1997 *J. Am. Chem. Soc.* **119** 7019
[10] Dabbousi B O, Rodriguez-Viejo J, Mikulec F V, Heine J R, Mattoussi H, Ober R, Jensen K F and Bawendi M G 1997 *J. Phys. Chem. B* **101** 9463
[11] Milliron D J, Hughes S M, Cui Y, Manna L, Li J, Wang L-W and Alivisatos A P 2004 *Nature* **430** 190
[12] Fischbein M D and Drndic M 2005 *Appl. Phys. Lett.* **86** 193106
[13] Klein D L, Roth R, Lim A K L, Alivisatos A P and McEuen P L 1997 *Nature* **389** 699
[14] Wolf S A, Awschalom D D, Buhrman R A, Daughton J M, von Molnár S, Roukes M L, Chtchelkanova A Y and Treger D M 2001 *Science* **294** 1488
[15] Coe S, Woo W-K, Bawendi M G and Bulović V 2002 *Nature* **420** 800
[16] Klimov V I, Mikhailovsky A A, Xu S, Malko A, Hollingsworth J A, Leatherdale C A, Eisler H-J and Bawendi M G 2000 *Science* **290** 314

[17] Reithmaier J P, Sęk G, Löffler A, Hofmann C, Kuhn S, Reitzenstein S, Keldysh L V, Reinecke T L and Forchel A 2004 *Nature* **432** 197
[18] Englund D, Fattal D, Waks E, Solomon G, Zhang B, Nakaoka T, Arakawa Y, Yamamoto Y and Vučković J 2005 *Phys. Rev. Lett.* **95** 013904
[19] Hennessy K, Badolato A, Winger M, Gerace D, Atatüre M, Gulde S, Fält S, Hu E L and Imamoğlu A 2007 *Nature* **445** 896
[20] Requicha A A G 2003 *Proc. IEEE* **91** 1922
[21] Castillo J, Dimaki M and Svendsen W E 2009 *Integr. Biol.* **1** 30
[22] Wang Z, Su S, Yang M, Fatikow S and Hülsen H 2007 *Proc. IEEE Intl. Conf. Mechatronics & Automation (Harbin, China)* p 422
[23] Fearing R S 1995 *Proc. IEEE/RSJ Intl Conf. Intelligent Robots and Systems (Pittsburgh, United States)* **2** 212
[24] Grier D G 2003 *Nature* **424** 21
[25] Moffitt J R, Chemla Y R, Smith S B and Bustamante C 2008 *Annu. Rev. Biochem.* **77** 205
[26] Salaita K, Wang Y and Mirkin C A 2007 *Nat. Nanotechnol.* **2** 145
[27] Voldman J 2006 *Annu. Rev. Biomed. Eng.* **8** 425
[28] Kolb J F, Joshi R P, Xiao S and Schoenbach K H 2008 *J. Phys. D: Appl. Phys.* **41** 234007
[29] Hamaker H C 1937 *Physica* **4** 1058
[30] Samara G A 1983 *Phys. Rev. B* **27** 3494
[31] Bergström L 1997 *Adv. Colloid Interface Sci.* **70** 125
[32] Hughes M P 2000 *Nanotechology* **11** 124
[33] Pohl H A 1978 *Dielectrophoresis (Cambridge University Press, Cambridge, UK)*
[34] Jones T B and Bliss G W 1977 *J. Appl. Phys.* **48** 1412
[35] Fernández D P, Mulev Y, Goodwin A R H and Levelt Sengers J M H 1995 *J. Phys Chem. Ref. Data* **24** 33
[36] Haus H A and Melcher J R 1989 *Electronamgnetic Fields and Energy (Prentice-Hall, Englewood Cliffs, United States)*
[37] Meinhart C, Wang D and Turner K 2003 *Biomed. Microdevices* **5** 139
[38] Löffler G, Schreiber H and Steinhauser O 1997 *J. Mol. Biol.* **270** 520
[39] Höfinger S and Simonson T 2001 *J. Comput. Chem.* **22** 290
[40] Knocks A and Weingärtner H 2001 *J. Phys. Chem. B* **105** 3635
[41] Li Y, Qian F, Xiang J and Lieber C M 2006 *Mater. Today* **9** 18
[42] Thelander C *et al.* 2006 *Mater. Today* **9** 28